Running title: Toward quantitative simulation of germinal center dynamics

Title: Toward quantitative simulation of germinal center dynamics. I. Biological and modeling insights from experimental validation.[1]

Authors: Steven H. Kleinstein[*†] and Jaswinder Pal Singh[*]

Keywords: Clonal Expansion, Repertoire Development, Spleen

ABSTRACT

Numerous *in vivo* and *in vitro* studies have elucidated the basic molecular mechanisms that underlie the germinal center reaction. However, it is still not well understood how these mechanisms fit together. Mathematical models can play an important role in solving this puzzle. Unfortunately, existing studies have either used models to explain qualitative, high-level behavior without comparing simulated dynamics with quantitative experimental data, or have presented validated models that do not simulate the underlying mechanism of selection, thus neglecting important constraints on germinal center dynamics. To truly understand the mechanisms and their interactions, as well as the validity of the hypotheses incorporated in models, comprehensive models must be validated by comparison with specific experimental data.

We examine whether a specific mathematical model of germinal center dynamics, proposed by Oprea and Perelson, can reproduce experimental data from the primary response to the hapten 2-phenyl-5-oxazolone. We develop a set of formulas for estimating response-specific model parameters, as well as a discrete/stochastic implementation of the Oprea and Perelson model that enables comparison with data on individual germinal centers. Based on the available data, we conclude that while the model can reproduce the average dynamics of splenic germinal centers, the model is at best incomplete and does not reproduce the distribution of individual germinal center behaviors. Thus, better understanding and improved models are needed. In addition to suggesting a possible extension to the model, we make a number of specific predictions that can be tested by *in vivo* experiments to obtain further insights and validation.

INTRODUCTION

Germinal centers play an important role in the immune response. They are the sites of affinity maturation where high-affinity B cells, formed through somatic mutation, are preferentially selected to proliferate. Numerous *in vivo* and *in vitro* studies have elucidated the basic molecular mechanisms that underlie the germinal center reaction. However, it is still not well understood how these mechanisms fit together. Mathematical models can play an important role in solving this puzzle and potentially in guiding experiments and making predictions.

A number of mathematical models have been developed to study affinity maturation (1-6). These can be roughly divided into two categories. In the first category fall those models which explicitly simulate the underlying mechanism of selection (e.g., B cells binding FDCs and/or T cells)[2] (1-4). These models make the important contribution of presenting high-level conclusions about the environment necessary for affinity maturation to occur; however, while the parameters of these models are often derived from or compared to experimental data, their emergent dynamics have not yet been carefully validated by comparing with experimental data. Models in the second category have been compared with experimental data (5, 6). However, these models neglect an important constraint on germinal center dynamics by simply assuming that higher-affinity cells are selected for at some pre-specified rate without simulating the underlying mechanism of this selection. Thus, existing studies either present models that have not been validated by comparing with experimental data, or validated models that do not simulate mechanism. To truly understand the mechanisms underlying the germinal center reaction and

their interactions, as well as the validity of the hypotheses incorporated in models, comprehensive models must be validated by comparison with specific experimental data.

For example, Oprea and Perelson have recently proposed a model of germinal center dynamics and affinity maturation (4). In this model dividing centroblasts undergo periodic rounds of affinity-based selection as non-dividing centrocytes. Significantly, Oprea and Perelson clearly represent the mechanism of selection: centrocytes die by apoptosis unless they can out-compete other cells and quickly bind to antigen held on FDCs. Using a differential equation-based simulation, Oprea and Perelson have shown that their model can achieve efficient affinity maturation if centrocytes recycle back to centroblasts. However, their model was not intended to reproduce the dynamics of any specific experimental system, but to describe the dynamics of a 'typical' immune response. It remains uncertain whether the results of the model can be applied to any particular real experimental system. In this study we attempt to validate the model by comparing its dynamics with data from the primary response to the hapten 2-phenyl-5-oxazolone (phOx). We choose this hapten because it evokes a relatively simple immune response and because a lot of experimental data is available for it.

In order to use the Oprea and Perelson (OP) model to simulate the phOx response, we must first provide estimates for the models parameters. One problem is that the affinity-class framework, used in the model to keep track of B cell affinities, is difficult to parameterize with experimental values since there is not a direct correspondence between framework parameters and experimentally measured values. We overcome this obstacle by providing formulas that explicitly convert experimental values to the parameters of the framework. It is also necessary to

choose one or more metrics that can be used to compare the dynamics of simulation versus experiment. For one, we propose a measure of the efficiency of affinity maturation among splenic germinal center B cells. This measure allows detailed quantitative comparison with sequence data collected from *in vivo* experiments. Additionally, we would like to utilize new data from studies that look at individual germinal centers in the spleen. As the differential equation-based simulation used in the Oprea and Perelson study deals only with bulk averages and is therefore unable to predict either individual germinal center behavior or the distribution of germinal center behaviors, we have developed a new discrete/stochastic implementation of the OP model[3]. Together, these tools allow us to ask precise questions about how well the model explains experimental observations.

The result of this validation process is a better understanding of the strengths and weaknesses of the OP model and where mechanisms or interactions must be better understood. In addition, we are able to make a number of specific predictions that can be tested by *in vivo* experiments to obtain further insights and validation.

EXPERIMENTAL SYSTEM & METHODS

The Oprea and Perelson model

The OP model describes the dynamics of the various germinal center cell populations including: B cell blasts, centroblasts, centrocytes, FDCs, centrocyte-FDC complexes and memory cells. It is defined by the following set of differential equations (4):

$$S(t) = S_0 e^{-d_S t} - \sum_i X_i$$

$$\frac{dB}{dt} = p_B B\left(1 - \frac{B}{M}\right) - \overbrace{k_d \Phi(t) B}^{\text{Flow1}}$$

$$\frac{dB_i}{dt} = \overbrace{k_d \Phi(t) B d_{i,0}}^{\text{Flow1}} + \overbrace{2 p_{Cb}\left[t(i,i)B_i + t(i-1,i)B_{i-1} + t(i+1,i)B_{i+1}\right] - p_{Cb}B_i}^{\text{Proliferate}} + \overbrace{p_R m_R R_i}^{\text{Exit}} - \overbrace{f_m B_i}^{\text{Flow2}} - d_B B_i$$

$$\frac{dC_i}{dt} = \overbrace{f_m B_i}^{\text{Flow2}} - \overbrace{k_f^i C_i S}^{\text{Bind}} + \overbrace{(1-r) k_r X_i}^{\text{Unbind}} - a C_i$$

$$\frac{dX_i}{dt} = \overbrace{k_f^i C_i S}^{\text{Bind}} - \overbrace{k_r X_i}^{\text{Unbind}}$$

$$\frac{dR_i}{dt} = \overbrace{r k_r X_i}^{\text{Unbind}} - \overbrace{m_R R_i}^{\text{Exit}} - d_R R_i$$

$$\frac{dM_i}{dt} = \overbrace{(1-p_R) h m_R R_i}^{\text{Exit}} - d_M M_i$$

$$\frac{dL_B}{dt} = \overbrace{2 p_{Cb} t_L \sum_i q_i B_i}^{\text{Proliferate}} - \overbrace{f_m L_B}^{\text{Flow3}} - a L_B$$

$$\frac{dL_C}{dt} = \overbrace{f_m L_B}^{\text{Flow3}} - a L_C$$

where,

$$f_m = m_0 + m_B \frac{L_B + \sum_i B_i}{L_B + \sum_i B_i + M_B}$$

and $\tau(i,j)$ is the probability that a centroblast in affinity-class *i* will move to affinity-class *j* upon division which includes mutation. The equations defining $\tau(i,j)$ are not shown here, but can be found in (4). A description of the variables is presented in Table I and the default parameter values can be found in Table II. In light of recent experimental studies (7), it is important to note that the model does not necessarily make any assumptions about germinal center architecture. However, the default values for some parameters (e.g., m_B and m_R) are based on the underlying

assumption that centroblasts are associated with the dark-zone and centrocytes with the light-zone.

Starting from the original OP model and its differential equation implementation, there are four challenges we need to overcome: (i) creating a discrete/stochastic simulation so that we can compare results with data collected from individual germinal centers, (ii) relating the parameters of the model to experimentally calculated values, (iii) dealing with affinities quantitatively, and (iv) metrics for validating the success of the model. In the following sections we deal with each of these in turn.

Creating the discrete/stochastic simulation

We have developed a discrete/stochastic implementation of the OP model in order to compare the dynamics with data collected from individual germinal centers. This implementation uses a *fixed-increment* time advance framework (8). Each simulation step updates the system dynamics through a fixed amount of time, Δt. To 'translate' the differential equation implementation into this discrete/stochastic framework, we first group related terms in the differential equations into independent processes (e.g., proliferation, death, binding, etc.). In the set of differential equations presented above, we have labeled all processes that span multiple equations. Each unlabeled term comprises its own process. These processes are combined together into a full simulation by performing them one after the other as part of each time step:

1. For each Δt from start to end

```
2.  For each process p
3.   Simulate p
4.  End for
5. End for
```

Since the order in which we perform the processes (line 2) matters, and in reality these processes are occurring in parallel, we simply perform the processes in a random order that changes each time-step. This hopefully avoids introducing too much bias into the simulation (e.g., as would happen if we always performed the proliferation process before death).

The discrete/stochastic framework is realized as follows. The variables in this framework represent cell numbers within an individual germinal center and are restricted to integer values. The rates on the right-hand-side of the differential equations are interpreted as probabilities of events occurring on individual cells during a time-step. This idea is easy to apply to processes that are confined to a single equation (e.g., all of the unlabeled terms in the above equations). As an example, consider the process modeling the apoptosis of centrocytes (i.e., the term $-\alpha C_i$). We model this as a Poisson process where the probability that one or more apoptosis 'events' occur during a particular time-step is $1-e^{-\alpha\Delta t}$. This will be valid as long as $\alpha\Delta t << 1$ which we can ensure by making the time-step small. The algorithm for simulating centrocyte apoptosis goes through all of the centrocytes in the germinal center, calculates the probability that apoptosis occurs during the time-step and then chooses a random number to decide whether apoptosis actually occurs for each individual centrocyte.

For processes which are spread across multiple equations, we must ensure that events are coordinated so that the total number of cells is conserved (where necessary). For example, consider the process labeled 'Unbind' which spans three equations. When a complex dissociates, the free B cell can either become a centrocyte (C_i) or a rescued centrocyte (R_i). Although the differential equation model has separate terms for the formation of centrocytes ($(1-r)k_r X_i$) and rescued centrocytes ($rk_r X_i$), we combine these in order to conserve the number of B cells. This can be specified by the following algorithm:

```
1. For all i
2.  For x = 1 to Xi
3.   If COIN(1−e^(−kr Δt)) then
4.    Xi = Xi - 1
5.    If COIN(ρ) then Ri = Ri + 1 else Ci = Ci + 1 End if
6.   End if
7.  End for
8. End for
```

where COIN(p) is a function that returns TRUE with probability p.

Variants of these algorithms are capable of handling all the rest of the processes.

Formulas to calculate parameters for the affinity-class framework

The OP model contains a number of parameters whose default values are not specifically based on the phOx system. For many of them, however, there is no evidence yet to suggest that their values would be significantly different during the phOx response. Exceptions to this are the parameters of the affinity-class framework, which describe the effect of somatic mutation on a B cell. The original study does not discuss how values for these parameters were derived; also, they do not correspond directly to experimentally observed values. In this section we overcome these shortcomings by extending the affinity-class framework with formulas to obtain the framework parameters from values that can be estimated directly from experimental data. We then derive estimates for these parameters that are consistent with the experimental system commonly used to study the phOx response (i.e., BALB/c mice immunized intraperitoneally with phOx coupled to the protein carrier chicken serum albumin) (9).

The affinity-class framework groups cells into a discrete number of affinity-classes $i \in \{..., -2, -1, 0, 1, 2, ...\}$ based on their affinity for antigen. Class 0 represents the germline affinity. The *affinity factor* controls the factor difference in on-rate between neighboring affinity-classes. The off-rate is assumed to be constant (a presumption that may be justified for the phOx response by the demonstrated importance of on-rates (10)). A non-lethal mutation may move a cell up or down a single affinity-class or may leave it in its current class. The relative probability of generating a lower- versus a higher-affinity mutant starting from affinity-class *i* is governed by the function $\Lambda(i)$, which is a user-specified parameter in the simulation. As specified in (4) and shown in Table II, the affinity-class framework requires a total of four parameters.

The affinity-class framework is an abstraction that equates a cell's affinity and genotype. It was first developed to avoid the problem of following and explicitly assigning affinities to each Ig genotype. This is an important feature, especially in modeling complicated responses, as it allows one to capture the qualitative features of the mutational landscape without knowledge of the quantitative details. Often, we will not know which specific sequences fall into each affinity-class or the effect of all possible mutations. While this generally makes experimental validation of a model that uses this framework difficult, the relative simplicity of the phOx response allows us to connect the affinity-class abstraction with a cell's genotype reasonably well. In particular, we interpret the affinity-class of a B cell as the number of affinity-increasing mutations in its Ig genes (relative to the germline sequence) minus the number of affinity-decreasing mutations. As we will see, this interpretation is not perfect, but it provides a good first approximation to the reality of the phOx response.

Given any starting sequence, we can express μ, the expressed mutation rate per division, in terms of the overall mutation rate and the number of base-pairs:

$$m = \hat{m} N p_e \qquad (1)$$

where $\hat{m}$ is the overall mutation rate per base-pair per division, N is the number of base-pairs that make up the Ig heavy and light chain genes and p_e is the fraction of mutations that are expressed, i.e. that cause a change in affinity-class.

Based on experimental data, $\hat{m} = 10^{-3}$ per base-pair per division (11) and $N = 681$ base-pairs (12). The fraction of mutations that are expressed, p_e, is simply the number of mutations that cause a change in affinity class divided by the total number of possible mutations:

$$p_e = \frac{n_1 + n_2 + n_3 + n_4}{N \times 3} \tag{2}$$

where $N \times 3$ is the total number of possible mutations (each nucleotide can mutate to one of 3 other bases) and:

n_1 = the number of mutations that are lethal (non-stop) framework replacements

n_2 = the number of mutations that are stop mutations

n_3 = the number of mutations that confer higher affinity

n_4 = the number of mutations that confer lower affinity, but are not lethal

Although the OP model assumes the same μ for all B cells, the precise value of p_e, and therefore of μ, will depend on the particular nucleotide sequence that is being mutated. Given a specific sequence, we can calculate μ by enumerating all possible mutations and counting how many of them fall into each of the four categories described above. Although n_1 and n_2 are probably almost constant, the values for n_3 and n_4 will almost certainly be different for B cells with different germline genotypes as well as for the same B cell at different stages of maturation. However, the case of phOx is greatly simplified by the fact that the primary response is dominated by a single germline encoded heavy/light chain combination (12). By restricting our simulation to follow only those B cells that carry this canonical germline sequence, we can

calculate a single initial value for μ. Also, since the average B cell accumulates only a small number of point mutations (13) and $n_1 + n_2 >> n_3 + n_4$ (see below), we should not be introducing too much error if we base our calculations on the germline sequence and ignore the fact that the value of μ will change as the B cell sequence changes under the influence of somatic mutation.

Starting from the canonical germline sequence, we find that $n_1 = 578$ based on the assumption that 50% of all framework replacements are lethal (14). Trivially, $n_2 = 96$. To calculate n_3, we rely on experiments that have shown that codon 34 of V_κ-Ox1 is highly selected for during the germinal center reaction. Mutation of this codon from the germline histidine to either glutamine or asparagine increases the affinity for phOx by about 10-fold (9). This single amino acid exchange accounts for most of the increase in affinity displayed by the best antibody seen by day 14 of the primary response (9). Thus, if we restrict our simulation to the first 14 days post-immunization, we find that there are only three mutations from the germline that lead to increased affinity (i.e., those leading to glutamine or asparagine at codon 34), so $n_3 = 3$. Finally, we assume that the number of affinity-decreasing mutations is directly related to the number of contact residues that make up the combining site between the canonical antibody and phOx. From structural studies of an antibody closely related to the canonical phOx antibody, it has been estimated that there are 14 contact residues (15). Since 7 out of the 9 possible mutations lead to replacements in the average codon in the CDR of the canonical antibody, we use $n_4 = 98$.

The mutations in categories n_1 and n_2 are lethal to the cell. Thus, the fraction of expressed mutations that are lethal to the cell, p_L, can be calculated as the number of mutations in these categories divided by the total number of expressed mutations:

$$p_L = \frac{n_1 + n_2}{n_1 + n_2 + n_3 + n_4} \tag{3}$$

Since there are only two known affinity-increasing amino acid exchanges in the phOx system, both at the same codon and both increasing the affinity by approximately 10-fold, we need only a single high-affinity class in our model. B cells in this high-affinity class will have a 10-fold higher affinity compared with the cells in the germline affinity-class. We will assume a constant affinity factor of A = 10, so that that this 10-fold affinity difference also carries to the lower affinity-classes.

The relative probability of generating a lower- versus a higher-affinity mutant from the germline affinity-class, $\Lambda(0)$, is given directly by the values of n_t calculated above (i.e., n_4/n_3). This can be extended to all affinity-classes with:

$$\Lambda(i) = \frac{n_4 + 7i}{n_3 - 3i}, i \in \{-13,...,-2,-1,0\} \text{ with } \Lambda(1) = \infty \text{ and } \Lambda(-14) = 0 \tag{4}$$

since each affinity-decreasing mutation that the cell accumulates means that there are 7 less mutations that decrease affinity (remember that *i* will be negative for cells that accumulate affinity decreasing mutations), and since each accumulated affinity-decreasing mutation implies the creation of, on average, 3 affinity-increasing mutations (i.e., reversions to the germline amino acid). Also, the minimum affinity-class is set to -14 reflecting the number of possible affinity-decreasing mutations[4].

Table II shows the parameter values for the phOx system that we calculated using the above formulas. Clearly, many assumptions were made in deriving parameters for the affinity-class framework. Nevertheless, since we are trying to validate the OP model which was expressed using this framework, we will use it in this paper. Interestingly, although the original Oprea and Perelson study did not specify how parameters for the affinity-class framework were determined, we can use the formulas developed in this section to retrofit assumptions for their study based on the (generic) parameter values they used. We find that the original parameter settings are equivalent to the assumption of 112 affinity-increasing mutations and 561 affinity-decreasing ones with a mutation rate of 2×10^{-4} per base-pair per generation.

A measure for the efficiency of affinity maturation

Similar to many previous mathematical models of affinity maturation (1, 3, 4), the Oprea and Perelson study uses the total affinity of the B cell population to quantify the extent of maturation. Although this measure provides an appropriate means to validate the model, it is virtually impossible to compare with experimental data since the model follows affinities at the cellular level while affinities are always measured experimentally at the thermodynamic level (i.e., using free antibody). It is not a simple matter to translate from one type of affinity measure to the other since one must account for avidity effects, the presence of co-receptors, cross-linking, signal transduction pathways, etc.

Instead of the total affinity, we define a new measure of affinity maturation F(*d*) as the fraction of B cells that are members of affinity-class 1, the high-affinity class, at day *d* in the simulated system. While this measure ignores the classification of cells in other affinity classes, we can directly compare it with experimentally collected sequence data since all B cells in the high-affinity class carry one of the high-affinity mutations at codon 34. An experimental estimate of F(*d*) is provided by (13). The estimate, $\Im(d)$, measures the accumulation of high-affinity mutations at codon 34 among splenic germinal center B cells (an average over many germinal centers). Table III summarizes this data which is available for days 10, 12 and 14 post-immunization. We can measure F(d) in the model as[5]:

$$F(d) = \frac{B_1(d) + C_1(d) + X_1(d) + R_1(d)}{B(d) + \sum_i \left(B_i(d) + C_i(d) + X_i(d) + R_i(d)\right)} \tag{5}$$

where descriptions of the variables can be found in Table I. When applying this formula to the discrete/stochastic simulation, each variable is the sum of 500 runs (i.e., approximately a spleens worth of germinal centers). In both the discrete/stochastic and the differential-equation simulations, F(*d*), like $\Im(d)$, represents the average dynamics of many germinal centers.

Comparing the efficiency of affinity maturation in simulation versus experiment

We define a quantitative measure of the fit between simulation and experiment, R^2, as the sum of the squares of the difference between F(*d*) and $\Im(d)$ for *d* = 10, 12 and 14:

$$R^2 = \sum_{d=10,12,14} \left(F(d) - \Im(d)\right)^2 \tag{6}$$

Lower values of R^2 indicate a better fit. In order to validate the model, we first set the values of any unknown parameters in such a way that R^2 is minimized. To do this, we have employed the downhill simplex method of Nelder and Mead (16). Next, we must decide whether the fit between model and experiment is good enough. It is highly unlikely, nor is it necessary, that we should find $F(d) = \Im(d)$. While we expect that $F(d)$ should give us the 'true' average, $\Im(d)$ is based on sampling a limited number of sequences. To estimate the error in $\Im(d)$, we have determined the 90% confidence interval based on the binomial distribution (17). We can rule out the model if $F(d) < \Im_{min}(d)$ or $F(d) > \Im_{max}(d)$, where $\Im_{min}(d)$ and $\Im_{max}(d)$ are the lower and upper bounds of the 90% confidence interval of $\Im(d)$ respectively.

RESULTS WITH THE DIFFERENTIAL EQUATION SIMULATION

The differential-equation simulation with default parameter values

In this section, we present the results from the differential equation simulation with all parameters set to their default values as specified in (4) except for those associated with the affinity-class framework which were set as described above. (Later, we will examine changing the other parameter values as well.) A list of these default parameter values is presented in Table II. Since k_{on} and k_{off} (the on and off rates for germline B cells) have not been measured experimentally (or estimated theoretically) we have estimated their best-fit values based on the fitness measure R^2. We find that the best fit with the experimental data occurs for $k_{on} = 0.01$ and $k_{off} = \infty$. This result would seem to rule out competition for antigen as a major pressure driving

affinity maturation. In order for competition to exist, B cells must remain bound to FDCs for some finite amount of time so they can prevent other cells from binding.

In order to further investigate this finding, we ran simulations for a range of germline k_{on} and k_{off}. The results (shown in Figure 1) reveal two main selection pressures that can drive affinity maturation in the OP model. Which pressure is operational depends on the germline affinity. For values of k_{on} around 10^{-2}, selection is driven by the fact that higher-affinity cells are more likely to escape from apoptosis. For higher values of k_{on} selection is the result of competition for binding to FDC sites. Affinity-dependent survival of apoptosis is not important in this latter case since all cells will have an on-rate sufficiently high to be rescued before apoptosis.

Under the default parameter values, affinity-dependent survival of apoptosis is the dominant selection pressure. The best-fit value of k_{off} is infinity since slower values simply prevent high-affinity cells from recycling without making selection any more stringent. Of course, an infinite off-rate is clearly not biologically realistic. We will later consider only $k_{off} \leq 100$. As shown in Figure 1, $k_{off} = 100$ can effectively be viewed as infinity since increasing k_{off} beyond this point does not provide a significantly better fit with the experimental data.

Regardless of the value of k_{off}, we find that affinity maturation with these parameter values is not strong enough to explain experimental observations. For example, the maximum value of F(14) is less than 15%. This is well below the 90% confidence interval of $36\% \leq \Im(14) \leq 71\%$. However, it does not follow immediately from this that the model is wrong. Default parameter values from (4) may be incorrect for the phOx response, or refinement of some aspects of the

model may be necessary. In the next section we will investigate possible changes to the model parameters that improve the efficiency of affinity maturation.

The differential equation simulation with revised parameter values

In this section, we broaden our search for parameter settings that can bring the model and experiment into agreement. Previously, we looked at varying only those parameters whose values were completely unknown (i.e., k_{on} and k_{off}). Which parameters should we now vary? The OP model has over a dozen parameters whose values have been estimated from experimental data and, without exception, each is associated with some degree of uncertainty. Unfortunately, methods for quantifying the precise degree of uncertainty do not currently exist. Thus, one cannot rigorously identify the weakest parameter estimates. This presents a real problem since a fit obtained by allowing all parameters to vary freely would almost certainly be suspect.

As a first step, we have identified those parameters that are based on the weakest assumptions or for which there is significant disagreement in the literature. We relied on numerous conversations with experimental immunologists as well as our own reading of the literature. Here, we highlight two different and independent hypotheses (i.e., changes to the default parameter settings) that bring simulation and experiment into agreement with respect to the fraction of splenic germinal center B cells that carry high-affinity mutations.

Hypothesis #1: The effective affinity factor is greater than ten.

The default value of the affinity factor, which controls the factor difference in on-rate between neighboring affinity-classes, rests on the questionable assumption that a B cell's affinity is a simple multiple of its surface immunoglobulin (sIg) affinity. Under this assumption, the experimentally observed 10-fold affinity increase at the antibody level translates directly into the modeled 10-fold increase at the cell level. In Figure 2, we show results from simulations that challenge this assumption by looking at a range of values for the affinity factor. According to these results, the smallest value of the affinity factor that can account for the experimental data is approximately 220. Although experimental evidence suggests that affinity differences at the antibody level will be diminished rather than amplified at the cell level (18), there is one possible way to reconcile an increased affinity factor in the model with biological reality.

T cells, which constitute about 5% of germinal center cells (19), are not explicitly part of the current model. However, in addition to the rescue signal from FDC, centrocytes probably need to get T cell help in order to avoid apoptosis (20). If the ability to secure T help were affinity-dependent (i.e., higher affinity B cells could strip more antigen from FDCs and therefore present themselves more effectively to T cells) then selection pressure on centrocytes could be increased. The overall effect of this can be simulated in the current model by increasing the affinity factor. However, without developing a more detailed model of T cells it is unclear what the magnitude of this increase should be. Even so, if we assume that the effect of T cells is well approximated by an increase in the affinity factor, then the maximum effect that T cells could have on affinity maturation is approximately given by the case where the affinity factor is 220; setting the affinity factor to a higher value does not help significantly since other processes become limiting.

Hypothesis #2: Division and migration parameters should be set to their most optimistic values

Even if the affinity factor remains set to its default value of 10, we can still match experimental data by changing other parameters. In Table IV we show evidence for four potential updates to the default parameter settings: an increased centroblast division and migration rate, an increased centrocyte migration rate and an increased capacity for the FDC network. To determine the impact of these changes, we ran a number of simulations that included all of the updates concurrently. The results (see Figure 3) show that these settings lead to a very good fit with the experimental data.

RESULTS WITH THE DISCRETE/STOCHASTIC SIMULATION

Using a discrete/stochastic simulation to study distributions

So far, we have been using a differential equation simulation, which models the average *ensemble* behavior of splenic germinal centers. However, recent experiments examining the accumulation of high-affinity mutations within *individual* germinal centers at day 14 have produced surprising results (21, 22). The most striking feature of the data is that the entire high-affinity population within each germinal center, if any, is descended from a single high-affinity mutant. Following the terminology of Radmacher *et al.* (6), we call the initial high-affinity mutant which gives rise to the observed lineage a *founder*. In addition, there is some evidence (summarized in Table V) for the *all-or-none* phenomenon that seems to be a characteristic of the NP response (6). That is, while many germinal centers produce no B cells with high-affinity

mutations, those that do are dominated by such cells by day 14. It is important to know if the OP model reproduces these observations.

We can test the model against these observations by using the discrete/stochastic implementation of the OP model. Unlike the differential equation simulation, which follows populations and uses the law of large number to suppress any deviations from the average behavior, the new simulation follows single B cells and takes into account the variation between individual germinal centers. This variation arises from timing differences among individual B cells in the occurrence of division, migration, apoptosis, etc. Another advantage of this discrete implementation is that it naturally handles all finite-size effects such as those recognized by (23) and corrected by the artificial threshold term $\boldsymbol{q}_i$ in the differential equation simulation. This threshold term prevents the growth of clones with a concentration of less than one B cell per germinal center.

For each hypotheses of the previous section, we performed 500 runs of the new simulation in order to simulate approximately a spleens worth of germinal centers. We define $F_x(d)$ as the fraction of B cells that are in the high-affinity class (class 1) on day d for a particular simulation run x that represents a single germinal center.

Testing Hypothesis #1: The effective affinity factor is greater than ten.

Figure 4 shows the results of simulations with an affinity factor of 220. In contrast to the experimental data, the high-affinity population within each germinal center cannot be traced

back to a single founder. Instead, an average of 6 cells per germinal center independently accumulate high-affinity mutations and produce progeny that persist to day 14. An additional 8 high-affinity lineages do not survive this long. Is it possible that multiple high-affinity lineages have not been observed in the experiments simply because of the small number of samples collected? Based on the experimental data, we have calculated that the observed high-affinity clone constitutes at least 96% of the high-affinity population ($p < 0.01$). In contrast, the simulation predicts that the founder with the greatest number of progeny will represent only slightly more than half of the high-affinity population at day 14. It is also easy to see that the simulation fails to reproduce the expected *all-or-none* phenomenon which would exhibit itself as a bimodal distribution in Figure 4.

Testing Hypothesis #2: Division and migration parameters should be set to their most optimistic values

We also used the discrete/stochastic simulation with the updated parameter set corresponding to higher division and migration rates and a larger germinal center size (but the default affinity factor) introduced in the previous section. Figure 5 presents the results of these simulations which are qualitatively similar to those found for hypothesis #1. On average, the high-affinity population at day 14 consists of the progeny of 18 founders out of 72 total high-affinity lineages. Furthermore, the founder with the greatest number of progeny represents only 27% of the high-affinity population. It is also easy to see that the simulation fails to reproduce the expected *all-or-none* phenomenon.

In both cases, the production of multiple founders and the failure to reproduce the *all-or-none* phenomenon stems from the fact that high-affinity clones are generated too early and too frequently (see Figure 6). Why don't we observe these clones experimentally? Radmacher *et al.* (6) suggest a possible reason. They have proposed that selection is a stochastic processes that "overlooks" many potential high-affinity founders. It is important to note that the simulations we have presented here already include many stochastic effects both in the initial generation and subsequent selection of high-affinity cells. However, the simulations show that their impact is significant only later in the response (Figure 6) by which point several high-affinity clones have already reached a large enough size that survival is virtually assured. Thus, additional stochastic mechanisms may have to be added in order to support the "overlooking" hypothesis.

Radmacher *et al.* (6), in fact, propose two mechanisms to make selection stochastic which are different from those already included in the OP model: cognate T/B cell interaction and preferential emigration of high-affinity cells. We can therefore add these to the model in order to see if they support the "overlooking" hypothesis. This can be accomplished by decreasing the probability of recycling which approximates the effect of these processes on germinal center dynamics. Indeed, we find that such mechanisms are able to lower the number of high-affinity founder cells to one (Figure 7). However, the efficiency of affinity maturation is drastically reduced in this case. This highlights an important insight. Affinity maturation in the OP model results only from the affinity-dependent selection of *centrocytes* since all centroblasts grow at the same rate regardless of their affinity. Thus, an expanded high-affinity clone must have survived a considerable number of selection events. Yet, the observation of a single high-affinity founder means that other high-affinity clones, created at nearly the same time, must have a low enough

probability of surviving selection that they are not observed. Thus, in the OP model, a stochastic selection mechanism cannot be responsible for limiting the number of high-affinity founder cells without reducing the efficiency of affinity maturation. For example, a high probability of selection leads to increased affinity maturation based on frequent recycling of high-affinity cells, but also allows a large number of founder cells to survive. In contrast, a low probability of selection drastically reduces both the number of founder cells and the efficiency of affinity maturation since few high-affinity survive to undergo additional proliferation.

To summarize the results of the discrete/stochastic simulations, neither of the two hypotheses that were able to explain the average ensemble dynamics of splenic germinal centers during the primary response to phOx was able to reproduce the experimental observations of individual germinal centers. Extending the model to include the suggestions of Radmacher *et al* did not help either, and they in fact highlighted an important aspect of the OP model that makes single-founder based affinity maturation unlikely to be observed without significant extensions to the model (i.e., more than just changing parameter values).

Avenues for additional validation experiments

In this section we list some additional predictions made by the OP model that can be tested experimentally. Understanding whether these predictions hold in real experiments will give us further, more specific insights into the validity of the model and hence the processes behind affinity maturation:

- Although no connection has yet been observed, the model predicts a positive correlation between the level of affinity maturation and germinal center size. This relationship is clearly seen in Figure 5 and, as best we can tell, takes the general form: $size = c^{F_x(14)}$ where c is a constant that depends on the particular model parameters under consideration. This correlation arises because effective division and survival rates are proportional to a cells affinity in the OP model.

- The model predicts that a B cell will quickly sense when it has accumulated a lethal mutation. Although no mechanism for detecting lethal mutations and hence triggering apoptosis prior to sIg expression is currently known, the OP model assumes that centroblasts with lethal mutations immediately begin apoptosis. If we instead assume that these mutations are only detected concurrently with the attempted expression of sIg (i.e., on differentiation to a centrocyte), we find that germinal centers are dominated by cells containing lethal mutations (data not shown).

- The OP model is highly sensitive to changes in the apoptosis rate. For example, while Figure 1 has the same general shape when the simulation is run with the apoptosis rate set to zero (data not shown), the overall level of affinity maturation is drastically reduced even when competition is the main force driving affinity maturation (i.e., at higher values of k_{on}). This is in seeming conflict with the experimental observation that interference with the apoptotic pathway through constitutive expression of bcl-2 does not affect affinity maturation (24).

- As discussed above, there are two main selection pressures that can drive affinity maturation in the OP model. This suggests two modes of affinity maturation (at least with respect to on-rates) depending on which selection pressure is operational. For apoptosis driven selection, affinity maturation will proceed quickly, but will also rapidly terminate as significantly higher on-rates cannot be selected for. In contrast, competition driven selection, although slower, can proceed as long as the necessary signals are available (e.g., Ag and T help). These two modes may provide an explanation for repertoire shift. The simulation data also clearly shows the existence of germline affinities for which affinity maturation will not occur.

DISCUSSION

Recently, Oprea and Perelson proposed a model of germinal center dynamics and affinity maturation during a 'typical' immune response (4). This model is noteworthy in that it explicitly describes the mechanism by which cells are selected for high-affinity binding to antigen. However, the model has never been applied to any specific experimental system and the extent to which it reflects biological reality, and solves the puzzle of affinity maturation, remains unclear. In order to better understand the model and its inherent assumptions, we have attempted to provide quantitative validation by comparing its dynamics with data from the primary response to the hapten 2-phenyl-5-oxazolone.

The original differential equation-based implementation of the OP model describes the *average* behavior of an ensemble of germinal centers. Under biologically realistic assumptions and

changing parameter values appropriately, this simulation can be made consistent with experimental data measuring the accumulation of high-affinity mutations among splenic germinal center B cells. However, the limitations inherent in models based on differential equations means that this correspondence ignores potentially important experimental results. For example, in order to compare the dynamics with the actual *distribution* of data collected from individual germinal centers, it was necessary to developed a discrete/stochastic implementation of the OP model. In contrast to the findings based on the original differential equation-based simulation, the results using this implementation showed that the OP model fails in two important ways. First, it cannot explain the observation of a single founder cell for the high-affinity population. Second, it does not reproduce the *all-or-none* phenomenon whereby germinal centers tend to either contain no high-affinity cells or are dominated by them.

The failure of the OP model stems from the fact that high-affinity founders are generated too early and too frequently. Although some of these high-affinity lineages are lost due to the randomness inherent in the selection process, too many still survive. Furthermore, it is not sufficient to simply extend the model by including additional stochastic components in the selection of high-affinity cells similar to those suggested by Radmacher *et al.* (6) for the NP response. In particular, decreasing the probability of selection reduces the number of founder cells only at the expense of affinity maturation. This relationship is, in fact, inherent in the OP model. As a possible solution, we propose further extending the OP model so that the mechanisms leading to the identification and initial selection of high-affinity cells are different from those leading to clonal dominance. For example, while the initial selection of a high-affinity cell may be dependent on binding to antigen and receiving T cell help, clonal dominance

may result from a higher division rate of this selected cell. Indeed, it has been estimated that the rate of take-over occurs at the same time-scale as cell division (6).

It is possible that our comparison with experimental data is confounded by the fact that by looking only at affinity the model may underestimate the number of cells that carry high-affinity mutations. This could happen, for example, if a cell gets a high-affinity mutation early and then subsequently accumulates one or more affinity-decreasing mutations at other positions. While such a cell would be included in the high-affinity population in experimental data, the simulation does not count such a cell as high-affinity. For this and a number of other reasons, we favor an approach where the simulation follows nucleotide sequences instead of affinities. As pointed out by Kepler and Perelson (2), this is not possible with standard differential equation-based simulations because of the large number of possible genotypes that must be followed. However, this problem can be overcome by using discrete simulations (which we have examined in this paper). In support of the current results, preliminary simulations using a sequence-based affinity model in place of the affinity-class framework produce values that are only about 10% higher than predicted here and with a similar distribution (data not shown).

In conclusion, our attempt to validate the OP model by comparing its dynamics with data from the primary response to phOx suggests that the Oprea and Perelson model in its current formulation is at best incomplete. However, we have proposed an extension to the model that should go a long way towards reconciling the model with experimental data. In addition, we have outlined a number of predictions of the OP model that can be tested experimentally. Other extensions to the OP model, or new models, that are capable of explaining the data on individual

germinal centers could also be investigated. Finally, although the dynamics of other hapten responses, such as NP, is similar to that of phOx, it would be useful to apply the model to these systems directly.

ACKNOWLEDGEMENTS

We thank Martin Weigert and Philip Seiden for their continual guidance and Alan Perelson for his help during a summer that S.H.K. spent working with him.

REFERENCES

1. Kepler, T. B., and A. S. Perelson. 1993. Cyclic re-entry of germinal center B cells and the efficiency of affinity maturation. *Immunol. Today 14:412*.
2. Kepler, T. B., and A. S. Perelson. 1993. Somatic Hypermutation in B Cells: An Optimal Control Treatment. *J. Theor. Biol. 164:37*.
3. Celada, F., and P. E. Seiden. 1996. Affinity maturation and hypermutation in a simulation of the humoral immune response. *Eur. J. Immunol. 26:1350*.
4. Oprea, M., and A. Perelson. 1997. Somatic Mutation Leads to Efficient Affinity Maturation When Centrocytes Recycle Back to Centroblasts. *J. Immunol. 158:5155*.
5. Shlomchik, M. J., P. Watts, M. G. Weigert, and S. Litwin. 1997. "Clone": A Monte-Carlo Computer Simulation of B Cell Clonal Expansion, Somatic Mutation and Antigen-Driven Selection. In *Curr. Top. Micro. Immunol.*
6. Radmacher, M. D., G. Kelsoe, and T. B. Kepler. 1998. Predicted and inferred waiting times for key mutations in the germinal centre reaction: Evidence for stochasticity in selection . *Immunol. Cell Biol. 76:373*.
7. Camacho, S. A., M. H. Kosco-Vilbois, and C. Berek. 1998. The dynamic structure of the germinal center. *Immunol. Today 19:511*.
8. Law, A. M., and W. D. Kelton. 1991. *Simulation modeling and analysis*. McGraw-Hill, Inc.
9. Berek, C., and C. Milstein. 1987. Mutation Drift and Repertoire Shift in the Maturation of the Immune Response. *Immunol. Rev. 96:23*.

10. Foote, J., and C. Milstein. 1991. Kinetic maturation of an immune response . *Nature 352:530*.

11. McKean, D., K. Huppi, M. Bell, L. Staudt, W. Gerhard, and M. Weigert. 1984. Generation of antibody diversity in the immune response of BALB/c mice to influenza hemagglutinin . *Proc. Natl. Acad. Sci. 81:3180*.

12. Kaartinen, M., G. M. Griffiths, A. F. Markham, and C. Milstein. 1983. mRNA sequences define an unusually restricted IgG response to 2-phenyloxazolone and its early diversification. *Nature 304:320*.

13. Berek, C., A. Berger, and M. Apel. 1991. Maturation of the Immune Response in Germinal Centers . *Cell 67:1121*.

14. Shlomchik, M. J., S. Litwin, and M. Weigert. 1990. The Influence of Somatic Mutation on Clonal Expansion . *Progress in Immunology. Proceedings of the Seventh International Congress of Immunology 7:415*.

15. Alzari, P. M., S. Spinelli, R. A. Mariuzza, G. Boulot, R. J. Poljak, J. M. Jarvis, and C. Milstein. 1990. Three-dimensional structure determination of an anti-2-phenyloxazolone antibody: the role of somatic mutation and heavy/light chain pairing in the maturation of an immune response. *EMBO. J. 9:3807*.

16. Press, W. H., S. A. Teukolsky, W. T. Vetterling, and B. P. Flannery. 1992. *Numerical Recipes in C*. Cambridge University Press, Cambridge.

17. Larsen, R. J., and M. L. Marx. 1986. *An introduction to mathematical statistics and its applications*. Prentice-Hall, New Jersey.

18. George, J., S. J. Penner, J. Weber, J. Berry, and J. L. Claflin. 1993. Influence of Membrane Ig Receptor Density and Affinity on B Cell Signaling by Antigen. *J. Immunol. 151:5955*.

19. Han, S., K. Hathcock, B. Zheng, T. B. Kepler, R. Hodes, and G. Kelsoe. 1995. Cellular Interaction in Germinal Centers. *J. Immunol. 155:556*.

20. Liu, Y.-J., D. E. Joshua, G. T. Williams, C. A. Smith, J. Gordon, and I. C. M. MacLennan. 1989. Mechanism of antigen-driven selection in germinal centers. *Nature 342:929*.

21. Ziegner, M., G. Steinhauser, and C. Berek. 1994. Development of antibody diversity in single germinal centers: selective expansion of high-affinity variants. *Eur. J. Immunol. 24:2393*.

22. Camacho, S. 1998. Temporal and Spatial Regulation of Affinity Maturation in the Primary Immune Response. Freien Universitat Berlin, Berlin, p. 112.

23. Kepler, T. B., and A. S. Perelson. 1995. Modeling and optimization of populations subject to time-dependent mutation. *Proc. Natl. Acad. Sci. USA 92:8219*.

24. Hande, S., E. Notidis, and T. Manser. 1998. Bcl-2 obstructs negative selection of autoreactive, hypermutated antibody V regions during memory B cell development. *Immunity 8:189*.

25. Zhang, J., I. C. M. MacLennan, Y.-J. Liu, and P. Lane. 1988. Is rapid proliferation in B centroblasts linked to somatic mutation in memory B cell clones. *Immunol. Lett. 18:297*.

26. Liu, Y., J. Zhang, P. J. L. Lane, E. Y.-T. Chan, and I. C. M. MacLennan. 1991. Sites of specific B cell activation in primary and secondary responses to T cell-dependent and T cell-independent antigens. *Eur. J. Immunol. 21:2951*.

27. Küppers, R., M. Zhao, M. L. Hansmann, and K. Rajewsky. 1993. Tracing B cell development in human germinal centers by molecular analysis of single cells picked from histological sections. *EMBO. J. 12:4955*.

Footnotes

---

[1] Supported in part by the National Science Foundation.

[*] Department of Computer Science, Princeton University, Princeton, NJ 08544

[†] Address correspondence and reprint requests to Steven Kleinstein, 35 Olden Street, Princeton, NJ 08544. E-mail address: stevenk@cs.princeton.edu

[2] Abbreviations used in this paper: CDR, complementarity determining region; FDC, follicular dendritic cell; GC, germinal center; OP, Oprea and Perelson; phOx, 2-phenyl-5-oxazolone; sIg, surface immunoglobulin

[3] A note on terminology: When we say "the model" or “the OP model,” we are referring to the conceptual model proposed by Oprea and Perelson. This model is defined by the set of differential equations in (4). Where necessary, we will refer to specific implementations of the model by saying "the differential equation simulation" or "the discrete/stochastic simulation".

[4] Actually, the minimum affinity class in the simulation is –3. The small number of cells that would populate the lower affinity classes do not effect the simulation dynamics.

[5] Note that this equation does not include centroblasts or centrocytes that have accumulated lethal mutations, members of L_B or L_C respectively.

Figure Legends

Figure 1: The effect of kon and koff on R2, the fitness measure between simulation and experiment. Results are shown for the differential equation simulation with default parameter values. The constrained best-fit parameter settings are indicated by the arrow (k_{on} = 0.01 and k_{off} = 100).

Figure 2: The effect of changing the affinity factor on R2, the fitness measure between simulation and experiment. For each value of the affinity factor, the best-fit with the experimental data was found by allowing k_{on} and k_{off} to vary with the constraint: $k_{off} \leq 100$. The thick dark portion of the line indicates settings that fit the experimental data according to a 90% confidence interval. The arrow marks the parameter values that we choose to exemplify hypothesis #1 (A = 220, k_{on} = 0.002 and k_{off} = 100).

Figure 3: The effect of changing the cell division and migration rates. Compares F(d), the average fraction of B cells that carry high-affinity mutations as predicted by the differential equation simulation, with the experimental estimate $\Im$(d) for the default (light line) and updated (dark line) parameter settings (described in Table IV). The error bars on the experimental measurements indicate the 90% confidence interval based on the limited number of samples collected. The best-fit with the experimental data was found by allowing k_{on} and k_{off} to vary with the constraint: $k_{off} \leq 100$. In both cases k_{on} = 0.01 and k_{off} = 100.

Figure 4: Testing hypothesis #1 with the discrete/stochastic simulation. The simulation was run 500 times to simulate approximately a spleens worth of germinal centers. The parameters, corresponding to hypothesis #1, included an increased affinity factor of 220 with k_{on} = 0.002 and k_{off} = 100. These simulations predict a value of F(14) = 39 $\pm$ 16%. The graph shows the distribution (bars) and cumulative distribution (solid line) of F_x(14) over individual germinal centers.

Figure 5: Testing hypothesis #2 with the discrete/stochastic simulation. The simulation was run 500 times to simulate approximately a spleens worth of germinal centers. The parameters, corresponding to hypothesis #2, included faster centroblast division (p_{Cb} = 4) and migration (m_B = 4), faster migration of

rescued centrocytes (m_R = 3.4) and increased FDC network capacity (M = 10^4) with k_{on} = 0.01 and k_{off} = 100. These simulations predict a value of F(14) = 48 $\pm$ 10%. (A) The distribution (bars) and cumulative distribution (solid line) of $F_x(14)$ over individual germinal centers. (B) The relationship between $F_x(14)$ and germinal center size at day 14.

Figure 6: The production and maintenance of high-affinity clones. Shows the cumulative number of distinct high-affinity clones produced (solid line) and the number of founder cells (i.e., those whose progeny are still present in the population) (dashed line) for hypothesis #2. The data represents an average of 500 simulation runs.

Figure 7: The effect of decreasing the probability of selection. Shows the number of high-affinity founder cells at day 14 (solid line) and R^2, the fitness measure between simulation and experiment (dotted line), for hypothesis #1. The data represents an average of 500 simulation runs.

Table I: The variables of the Oprea and Perelson model of the germinal center as defined in (4).

Variable	Description
S	Free FDC sites
B	B cell blasts
B_i	Centroblasts in affinity-class *i*
C_i	Centrocytes in affinity-class *i*
X_i	Centrocyte-FDC complexes where the centrocyte is in affinity-class *i*
R_i	Rescued centrocytes in affinity-class *i*
M_i	Memory B cells in affinity-class *i*
L_B	Centroblasts with lethal mutations
L_C	Centrocytes with lethal mutations

Table II: Default parameter values. (A) The parameters of the affinity-class framework along with their default values calculated to model the immune response to phOx. Original values, taken directly from (4), are shown for comparison. (B) The rest of the model parameters with default values as specified in (4).

A.

Parameter	Description	Original Value	phOx Value
m	Expressed mutation rate per genome per division	0.1	0.26
p_L	Fraction of expressed mutations that are lethal	0.5	0.87
$\Lambda(i)$	Relative probability of generating a lower vs. higher affinity mutant starting from affinity-class *i*	$\Lambda(0)$ = 5.0	$\Lambda(0)$ = 32.7
A	Factor difference in on-rate between neighboring affinity-classes	5	10

B.

Parameter	Description	Default Value
$B_0(0)$	Number of B blasts that seed the GC	3 B cells
	Day when GC is seeded	3
S_0	Initial number of FDC sites	300
$1/d_S$	Average lifetime of FDC sites	30 $days^{-1}$
P_B	Maximum proliferation rate of B blasts	3 $days^{-1}$
k_d	Maximum rate that B blasts convert to centroblasts	6 day^{-1}
P_{Cb}	Centroblast proliferation rate	2.5 day^{-1}
M	Capacity of the FDC network	1500 B cells
M_B	Saturation constant for centroblast migration	500 B cells
d_R	Death rate of rescued centrocytes	0.03 day^{-1}
d_M	Death rate of memory cells	0.03 day^{-1}

d_B	Death rate of centroblasts	0.3 day^{-1}
α	Apoptosis rate	4 day^{-1}
p_r	Probability of recycling	0.7
η	Proportion of cells that exit GC that become memory cells	0.1
m_B	Migration of centroblasts, maximal rate	2.5 day^{-1}
m_0	Migration of centroblasts, baseline rate	0.3 day^{-1}
m_R	Rescued centrocyte migration rate	2.5 day^{-1}
k_{on}	on-rate for germline B cell / FDC binding	-
k_{off}	off-rate for germline B cell / FDC dissociation	-
ρ	Probability of a bound centrocyte being rescued	0.8

Table III: The fraction of splenic germinal center B cells carrying high-affinity mutations at day 14 as summarized from *(13)*. V_κ-Ox1 sequences were amplified by using PCR on the PNA^{hi} subset of splenic B cells. $\Im(d)$ measures the fraction of PCR products that carry one of the high-affinity mutation at codon 34 at day d. $\Im_{min}(d)$ and $\Im_{max}(d)$ are the lower and upper bounds of the 90% confidence interval respectively.

	Sequences Analyzed	$\Im(d)$	$\Im_{min}(d)$	$\Im_{max}(d)$
Day 10	18	6%	0.3%	24%
Day 12	11	27%	8%	56%
Day 14	26	54%	36%	71%

Table IV: Updates to the default parameter settings proposed by hypothesis #2. These changes are based on the most optimistic values proposed in the literature.

Quote	Reference	Default	Updated
"The present report provides evidence pointing to centroblasts having a remarkably short cell cycle time of 6 to 7 hours."	(25)	$p_{Cb} = 2.5$ $m_B = 2.5$	$p_{Cb} = 4.0$ $m_B = 4.0$
"…the centrocyte population is renewed from centroblasts every 7h."	(26)*	$m_R = 2.5$	$m_R = 3.4$
"…we estimate that [the germinal centers] contain ≈1 x 10^4 B cells each."	(27)**	M = 1500	M = 10^4

* used rats (not mice) in a carrier primed response (i.e., T help is non-limiting)

** used germinal centers from human lymph nodes

Table V: The fraction of cells carrying high-affinity mutations at day 14 within individual germinal centers as summarized from *(21)* and (22). Ten germinal centers (not shown) produced no high-affinity cells. Individual germinal centers were dissected from frozen spleen sections and V_κ-Ox1 sequences were amplified by PCR. $\Im_x(14)$ measures the fraction of PCR products that carry one of the high-affinity mutations at codon 34 at day 14.

GC	# Sequences	$\Im_x(14)$
Q	61*	3%
7A	21	29%
N	30	67%
E	20	85%
III-1	11	100%
III-2	73	100%

*Three different V_κ-Ox1 rearrangements were found in this germinal center

Figure 1: The effect of k_{on} and k_{off} on R^2, the fitness measure between simulation and experiment.

A.

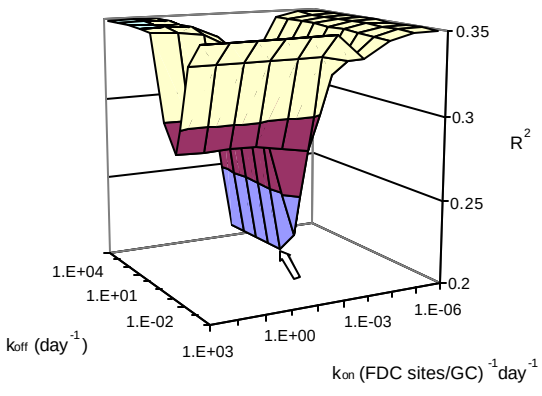

Figure 2: The effect of changing the affinity factor on R^2, the fitness measure between simulation and experiment.

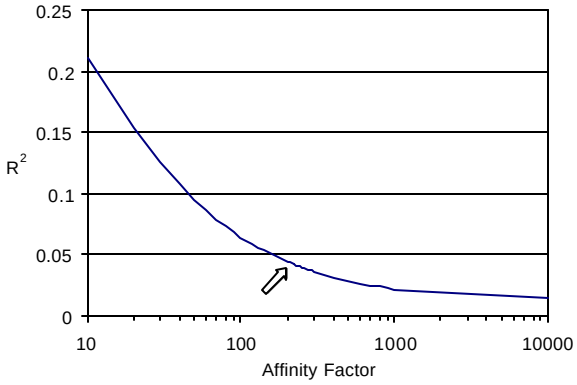

Figure 3: The effect of changing the cell division and migration rates.

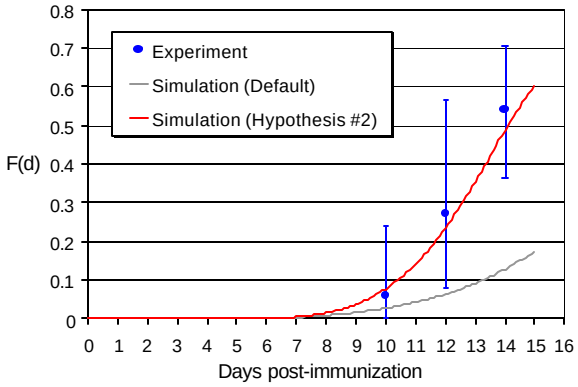

Figure 4: Testing hypothesis #1 with the discrete/stochastic simulation.

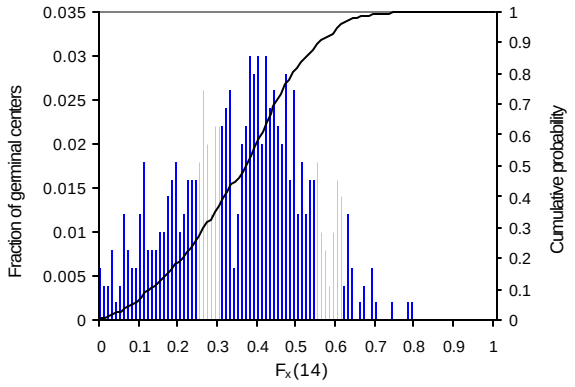

Figure 5: Testing hypothesis #2 with the discrete/stochastic simulation.

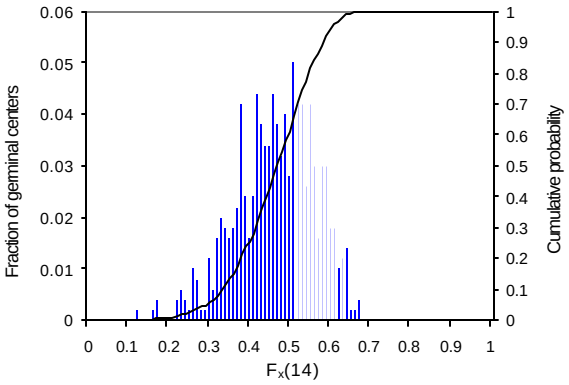

A.

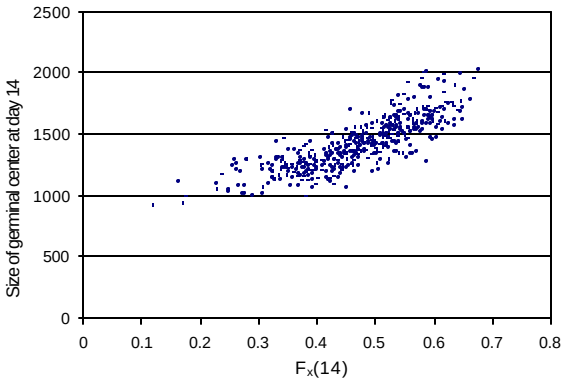

B.

Figure 6: The production and maintenance of high-affinity clones.

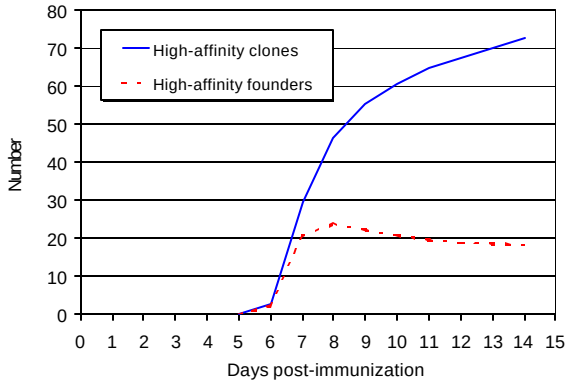

Figure 7: The effect of decreasing the probability of selection.